Pramāṇa, Vol. 3, No. 4, 1974, pp 243-260. © Printed in India.

# In-beam gamma-ray and electron spectroscopy following the $^{75}$As(p, n)$^{75}$Se reaction

Y K AGARWAL*, C V K BABA†, S M BHARATHI*,
S K BHATTACHERJEE*, B LAL* and BALDEV SAHAI*
* Tata Institute of Fundamental Research, Bombay 400005
† Nuclear Physics Division, Bhabha Atomic Research Centre, Bombay 400085

MS received 18 April 1974

**Abstract.** The level scheme of $^{75}$Se has been studied through the $^{75}$As (p, n) reaction at proton energies from 1·5 to 5·0 MeV. $\gamma$-ray and internal conversion electron measurements were made using NaI (Tl) and Ge (Li) detectors and a six-gap electron spectrometer. A proportional counter and a thin window NaI (Tl) detector were used to detect $\gamma$-rays with energies less than 30 keV. The level scheme has been established by observing the thresholds of various $\gamma$-rays and by $\gamma$–$\gamma$ and $e^-$–$\gamma$ coincidence measurements. New levels at 133·0, 293·2, 790·0, 953·0, 1020·8, 1184·3, 1198·5 and 1258·2 keV not observed in earlier (p, n) studies have been established. Conversion coefficients of most of the low-lying transitions have been determined. Angular distributions of some of the $\gamma$-rays were also measured and compared with the statistical model calculations. Definite $J^\pi$ assignments have been made to most of the low-lying levels. Life-times of the 112·1, 133·0, 286·7 and 293·2 keV levels have been measured to be $0{\cdot}69 \pm 0{\cdot}12$, $5{\cdot}3 \pm 0{\cdot}6$, $1{\cdot}35 \pm 0{\cdot}15$ and $31 \pm 2$ nsec respectively. The reduced transition probabilities for various low-lying transitions have been determined and compared with recent calculations. The $1/2^-$ and $9/2^+$ levels hitherto unknown in this nucleus have been identified. The structure of the low-lying levels is discussed in terms of the existing models.

**Keywords.** Nuclear reaction $^{75}$As (p, n) $^{75}$Se; $\gamma$-ray angular distribution; nuclear structure; deformation; internal conversion coefficients.

## 1. Introduction

In nuclei with $N = 40$–50, the valence neutrons should occupy the $p_{1/2}$ and $g_{9/2}$ orbitals according to the single particle model. Both theoretically and experimentally, this region has not been studied in detail mainly due to the complexity of the level schemes. Odd neutron nuclei in this region show low-lying $7/2^+$ and $5/2^+$ states in addition to the expected negative parity states; the $9/2^+$ state has not been identified in all the nuclei in this region. In $^{75}_{34}Se_{41}$, the ground state spin is $5/2^+$ (Aamadt and Fletcher 1955). When this work was taken up, the $9/2^+$ and the $1/2^-$ levels in this nucleus had not been identified. The level scheme of this nucleus has been studied by several groups. Finckh *et al* (1970) studied the levels by a neutron time-of-flight study of the reaction $^{75}$As(p, n)$^{75}$Se ($Q = -1{\cdot}65$ MeV), while Richter *et al* (1968) and Tubbs (1966) studied the $\gamma$-rays following the reaction. Ray *et al* (1969), Dzhelepov *et al* (1969, 1970),

Ladenbauer-Bellis and Bakhru (1969) and Coban *et al* (1972) have studied the electron-capture decay of the $3/2^-$ ground state of $^{75}$Br in detail. Some information has resulted from the study of the (d, p) reaction of $^{74}$Se by Litvin *et al* (1968). Rudak *et al* (1970) have studied some of the levels in $^{75}$Se populated by thermal-neutron capture in $^{74}$Se. After this work was completed, Sanderson (1973) reported a study of the $^{76}$Se (d, t) $^{75}$Se reaction. Recently evidence has been presented to suggest that $^{75}$Se and some other odd mass nuclei in this region are deformed (Baba *et al* 1974).

The present work was undertaken to locate the $g_{9/2}$ and the $p_{1/2}$ levels and to study the electromagnetic decay properties of the low-lying levels in $^{75}$Se in order to throw more light on the anomalous coupling scheme (Sherwood and Goswami 1966) encountered in this region. A detailed study of the $\gamma$-ray and internal conversion electron spectra following the $^{75}$As (p, n) $^{75}$Se reaction has been made. In addition, lifetimes of several low-lying levels and angular distributions of some $\gamma$-rays have been measured. As a result of this study, low-lying $1/2^-$ and $9/2^+$ levels have been identified and information has been obtained on the electromagnetic decay properties of the low-lying levels in $^{75}$Se. Preliminary account of this work has been reported earlier (Sahai and Lal 1970, Lal and Sahai 1972, Agarwal *et al* 1973).

## 2. Experimental details

The experiments were performed using the 5·5 MeV Van de Graaff accelerator at the Bhabha Atomic Research Centre, Bombay. The relevant experimental details are given below.

### 2.1. *Target preparation*

Two types of targets were used in the experiment. Thin targets ($\simeq 100\,\mu g\ cm^{-2}$) made by vacuum evaporation of spectroscopically pure arsenic obtained from the Chemistry Division of BARC onto thin ($\simeq 50\,\mu g\ cm^{-2}$) carbon backing were used for most of this work. Thick targets (1 cm × 2 mm thick) made by pressing arsenic metal powder in a steel mould in a 10 ton hand press were used for excitation function and $\gamma$–$\gamma$ coincidence measurements.

### 2.2. *$\gamma$-ray spectroscopy*

Several NaI (Tl) and Ge (Li) detectors were used to study the $\gamma$-ray spectra. The NaI (Tl) detectors were used mainly for $\gamma$–$\gamma$ coincidence and lifetime measurements. A thin window NaI (Tl) and a proportional counter were used to detect low energy $\gamma$-rays. Two Ge (Li) detectors, a 30 cm$^3$ 'coaxial' supplied by Nuclear Diodes, USA and a 4 cm$^3$ 'planar' made in our laboratory (Deshpande 1971), were used for high-resolution study of $\gamma$-ray spectra. The 4 cm$^3$ detector, used along with the electron spectrometer, could be placed at a distance of 4 cm from the target. This arrangement enables a simultaneous measurement of internal conversion spectra and $\gamma$-ray spectra and thus accurate measurements of internal conversion coefficients can be made even with targets which deteriorate with time due to beam heating. The 30 cm$^3$ Ge (Li) detector was used for detailed $\gamma$-ray spectroscopy. For threshold determinations, $\gamma$-ray spectra were recorded using 'pellet' targets and proton energies in the range 1·5–3·8 MeV in approximately

200 keV steps. A few spectra were recorded using 'thin' targets and proton energies in the range 2·3–4·5 MeV. The computer code SAMPO (Routti and Prussin 1969) adapted to the CDC 3600 computer at TIFR was used to analyze the $\gamma$-ray spectra. Relative efficiency and energy calibrations for the detector were obtained by recording $\gamma$-ray spectra from standard radioactive sources ($^{152}$Eu, $^{137}$Cs, $^{133}$Ba and $^{22}$Na) and using the relative intensities as given by Greenwood *et al* (1970). $\gamma$–$\gamma$ coincidence spectra were recorded with the 'pellet' target using the 30 cm$^3$ Ge (Li) detector and a 5 cm × 2·5 cm NaI (Tl) detector. The resolving time of the coincidence circuit was $\simeq$ 80 nsec. Narrow energy windows were selected in the NaI (Tl) counter spectra using a single channel analyzer and coincident Ge (Li) spectra were recorded in the multichannel analyzer. The observed spectra were corrected for random events. Spectra were also obtained by shifting the single channel analyzer window off the photopeaks. The corrected coincidence spectra were quantitatively analyzed to derive the branching ratios and the decay scheme.

### 2.3. *Internal conversion electron spectroscopy*

A six gap "Orange" electron spectrometer with $\simeq$ 7% transmission at $\simeq$ 1% resolution was used for internal conversion electron spectroscopy. This spectrometer is similar to that described by Bisgaard (1963). To facilitate beam alignment, the spectrometer is provided with levelling screws and is installed on a movable stand. The proton beam from the accelerator passes through a soft-iron tube located between two gaps. This reduces beam bending in the field of the spectrometer. After passing through the 'thin' target, the beam is stopped in a well-shielded Faraday Cup. A 2·5 cm × 1·2 cm anthracene crystal coupled to a low noise EMI 9536 SA photomultiplier was used to detect the electrons. A Philips 56 AVP photomultiplier and a NE 211 plastic scintillator were used for measuring short half-lives (*see* section 2.5). The 4 cm$^3$ Ge (Li) detector was mounted on top of the spectrometer to record the $\gamma$-ray spectra. In order to minimize the angular distribution effects in the measured $\gamma$-ray spectra, the Ge (Li) detector was located at an angle of 60° with respect to the beam direction. The normalisation factor required for the computation of internal conversion coefficients was determined by recording the $\gamma$-ray and conversion electron spectra of the well-known 190 keV E3 transition in $^{81}$Kr produced by the reaction $^{81}$Br(p, n) $^{81}$Kr and making use of the theoretical value of internal conversion coefficient ($\alpha_k$) for this transition (Hager and Seltzer 1968). A short description of the spectrometer has already been published by Ambardekar *et al* (1969).

### 2.4. *Angular distribution of $\gamma$-rays*

In order to get some information on spins of the low-lying levels, measurements of the angular distributions of some of the $\gamma$-rays were made. The 30 cm$^3$ Ge (Li) detector kept at a distance of 7 cm from the target could be rotated around the target position. A 5 cm × 2·5 cm NaI (Tl) detector kept at 90° with respect to the beam direction and at a distance of 10 cm from the target was used as a fixed monitor and the Ge (Li) spectra recorded at various angles were suitably normalised. Since one of the requirements of the applicability of statistical theory to the

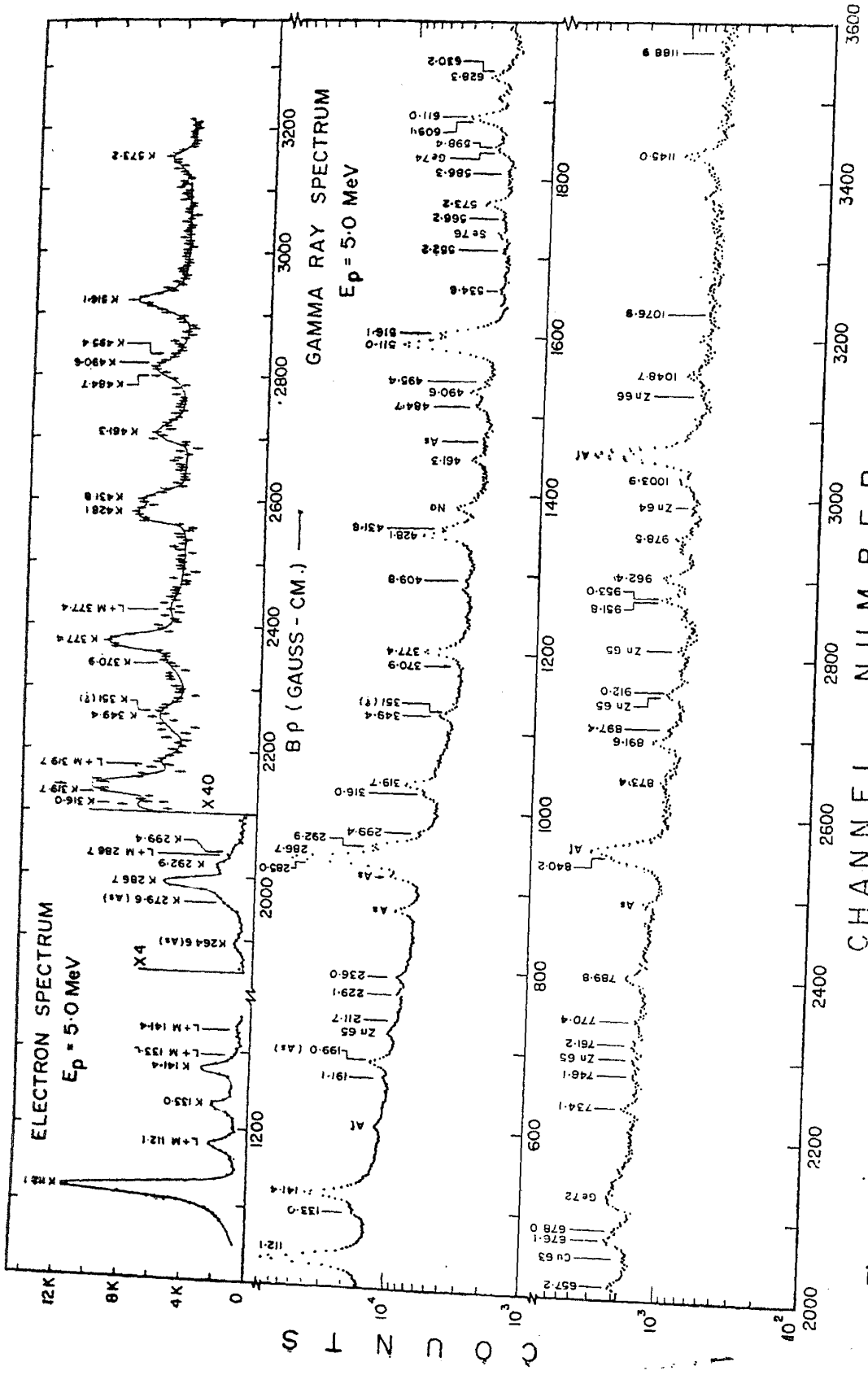


**Figure 1.** The conversion electron spectrum recorded with the six gap electron spectrometer and the $\gamma$-ray spectrum recorded with a 30 cm$^3$ Ge (Li) detector obtained by proton bombardment of a 100 $\mu$g cm$^{-2}$ As target at $E_p = 5{\cdot}0$ MeV. The numbers indicate the energies of the lines in keV. The lines other than those from $^{75}$As(p, n)$^{75}$Se reaction are appropriately marked.

angular distribution studies is that a large number of levels in the compound nucleus be excited, the targets used in the angular distribution measurements were $\simeq 300$ $\mu g$ $cm^{-2}$ ($\simeq 20$ keV for 2·5 MeV protons) thick and consisted of four 'thin' targets stacked together. This requirement was also met with by measuring the angular distributions at two proton energies differing by 20 keV. The measurements were made at proton energies $\simeq 100$ keV above the thresholds in order to have a predominant $l = 0$ contribution in the outgoing neutron channels. This causes the angular distributions to be almost independent of the optical model parameters used for calculating the transmission coefficients. The experimental angular distributions were compared with the theoretical expressions given by Sheldon and Van Patter (1966). Elastic, and all possible inelastic and neutron exit channels for the decay of the compound nucleus were considered. Orbital angular momenta up to $l = 5$ were used in the incoming and outgoing channels. The transmission coefficients for the neutrons and protons were calculated using the code ABACUS (Auerbach 1964) and the optical model parameters given by Rosen *et al* (1965) for protons and Wilmore and Hodgson (1964) for neutrons. A computer code HFMODEL written for the CDC 3600 Computer was used for the statistical model calculations.

### 2.5. *Lifetime measurements*

The lifetime measurements were carried out by recording time-spectra between transitions feeding and deexciting levels of interest. $e^- - \gamma$ or $\gamma - e^-$ or $n - e^-$ cascades were used for this purpose. The $\gamma$-rays were detected either in a NaI (Tl) or a plastic detector. By using internal conversion electrons in the lifetime measurements, background events caused by Compton scattering, normally present under the peaks in question were eliminated. Two constant-fraction trigger circuits and a fast time-to-amplitude converter (TAC) were used for these measurements. The TAC was calibrated by measuring the well-known lifetimes of the 122 keV level in $^{152}Sm$ and the 81 keV level in $^{133}Cs$.

## 3. Results

A $\gamma$-ray spectrum from a 'thin' target bombarded with protons of energy $E_p = 5{\cdot}0$ MeV and recorded with the 30 $cm^3$ Ge (Li) detector is shown in figure 1. The $\gamma$-ray energies are marked in the figure. The lines marked 'As' were identified as due to Coulomb excitation and (p, p′) reaction on $^{75}As$. The energies, thresholds and the assignments in the level scheme for various $\gamma$-transitions are given in table 1. Figure 1 also shows an internal conversion electron spectrum taken at $E_p = 5{\cdot}0$ MeV. The values of $\alpha_k$ for the various transitions determined as outlined in section 2.3 are given in table 1. In figure 2, the measured internal conversion coefficients are compared with the theoretical values (Hager and Seltzer 1968) and the multipolarities of the different transitions are deduced. Further, angular distributions of the 112·1, 141·4 and the 377·4 keV transitions were measured. Figure 3 shows the results for the 112·1 and 377·4 keV transitions along with the $\chi^2$ plots. From these measurements, the spins of the 112·1 and 664·1 keV levels are found to be 7/2 and 5/2 respectively, and for the 428·1 keV levels two values, 7/2 and 5/2, are allowed. A summary of the $\gamma$-$\gamma$ coincidence measurements is given in table 2. From the threshold measurements, energy sum relations

**Table 1.** List of $\gamma$-rays from the reaction As (p, n) at $E_p = 3{\cdot}5$ MeV

| $E^{(a)}$ (keV) | Threshold$^{(b)}$ $E_p$ (MeV) | Assignment$^{(c)}$ (keV → keV) | $\alpha_k{}^{(d)}$ |
|---|---|---|---|
| 6·5 | .. | 293·2 → 286·7 | |
| 20·9 | .. | 133·0 → 112·1 | |
| 112·1 | 1·95 | 112·1 → 0 | 9·2 ± 1·0 (−2) |
| 133·0 | 2·40 | 133·0 → 0 | 2·7 ± 0·3 (−1) |
| 141·4 | 2·24 | 428·1 → 286·7 | 3·5 ± 0·4 (−2) |
| 191·1 | 2·54 | 777·5 → 586·1 | |
| 211·7 | 2·65 | 840·0 → 628·2 | |
| 229·1 | 2·65 | 840·0 → 611·0 | |
| 236·0 | 2·40 | 664·1 → 428·1 | |
| 285·0 | 2·80 | 1074·7 → 790·0 | |
| 286·7 | 2·10 | 286·7 → 0 | 3·1 ± 0·2 (−3) |
| 292·9 | 2·30 | 586·1 → 293·2 | 5·9 ± 0·4 (−3) |
| 299·4 | 2·30 | 586·1 → 286·7 | 6·2 ± 1·8 (−3) |
| 316·0 | 2·24 | 428·1 → 112·1 | |
| 319·7 | 2·50 | 748·0 → 428·1 | |
| 349·4 | 2·54 | 777·5 → 428·1 | 3·5 ± 1·3 (−3) |
| 370·9 | .. | 664·1 → 293·2 | 5·3 ± 2·0 (−3) |
| 377·4 | 2·40 | 664·1 → 286·7 | 2·8 ± 0·5 (−3) |
| 409·8 | 3·25 | (1020·8 → 611·0) | |
| 428·1 | 2·24 | 428·1 → 0 | 1·1 ± 0·1 (−3) |
| 431·8 | 2·65 | 859·7 → 428·1 | 2·4 ± 0·4 (−3) |
| 461·3 | 2·65 | 748·0 → 286·7 | 3·2 ± 0·5 (−3) |
| 484·7 | 2·54 | 777·5 → 293·2 | |
| 490·6 | 2·54 | 777·5 → 286·7 | |
| 495·4 | 2·49 | 628·2 → 133·0 | |
| 516·1 | 2·49 | 628·2 → 112·1 | 1·3 ± 0·2 (−3) |
| 534·6 | 2·70 | 962·6 → 428·1 | |
| 552·2 | 2·80 | 664·1 → 112·1 | |
| 566·2 | .. | 859·7 → 293·2 | |
| 573·2 | .. | 859·7 → 286·7 | 1·6 ± 0·4 (−3) |
| 586·3 | 2·30 | 586·1 → 0 | |
| 598·4 | .. | 1184·3 → 586·1 | |
| 609·1 | 2·80 | 895·8 → 286·7 | |
| 611·0 | 2·30 | 611·0 → 0 | |
| 628·3 | 2·49 | 628·2 → 0 | |
| 630·2 | 3·00 | 1258·2 → 628·2 | |
| 657·2 | .. | 790·0 → 133·0 | |
| | | $^{75}$As (p, $\gamma$) $^{76}$Se | |
| 676·1 | 2·80 | 962·6 → 286·7 | |
| 678·0 | 2·60 | 790·0 → 112·1 | |
| 734·1 | 2·80 | 1020·8 → 286·7 | |
| 748·1 | 2·54 | 748·0 → 0 | |
| 761·2 | .. | 1189·1 → 428·1 | |
| 770·4 | .. | 1198·5 → 428·1 | |
| 789·8 | 2·60 | 790·0 → 0 | |
| 840·2 | .. | 840·0 → 0 | |
| 873·4 | 3·10 | 1301·3 → 428·1 | |
| 891·6 | 2·80 | 1003·7 → 112·1 | |
| 897·4 | 3·00 | 1184·3 → 286·7 | |

**Table 1.** (*Contd.*)

| $E^{(a)}$ (keV) | Threshold$^{(b)}$ $E_p$ (MeV) | Assignment$^{(c)}$ (keV → keV) | $\alpha_K{}^{(d)}$ |
|---|---|---|---|
| 912·0 | 3·00 | 1198·5 → 286·7 | |
| 951·8 | .. | 1245·1 → 293·2 | |
| 953·0 | 2·70 | 953·0 → 0 | |
| 962·4 | 2·70 | 1074·7 → 112·1 | |
| | | 962·6 → 0 | |
| 978·5 | 3·25 | 1406·6 → 428·1 | |
| 1003·9 | 2·80 | 1003·7 → 0 | |
| 1048·7 | 3·00 | 1160·8 → 112·1 | |
| 1076·9 | 3·00 | 1189·1 → 112·1 | |
| 1145·0 | 3·00 | 1145·0 → 0 | |
| 1188·9 | 3·10 | 1301·3 → 112·1 | |
| | | (1189·1 → 0) | |
| 1245·1 | 3·00 | 1245·1 → 0 | |
| 1257·7 | 3·10 | 1258·2 → 0 | |
| 1301·4 | 3·10 | 1301·3 → 0 | |
| 1379·4 | 3·25 | 1379·4 → 0 | |
| 1437·6 | 3·25 | 1437·6 → 0 | |

(*a*) The error on the energies for most of the transitions are less than ± 0·4 keV.
(*b*) The lowest proton energy at which the particular transition was observed.
(*c*) The transitions shown in brackets do not have a very definite place in the decay scheme.
(*d*) The numbers in the bracket in this column indicate the power of the multiplicative factor 10.

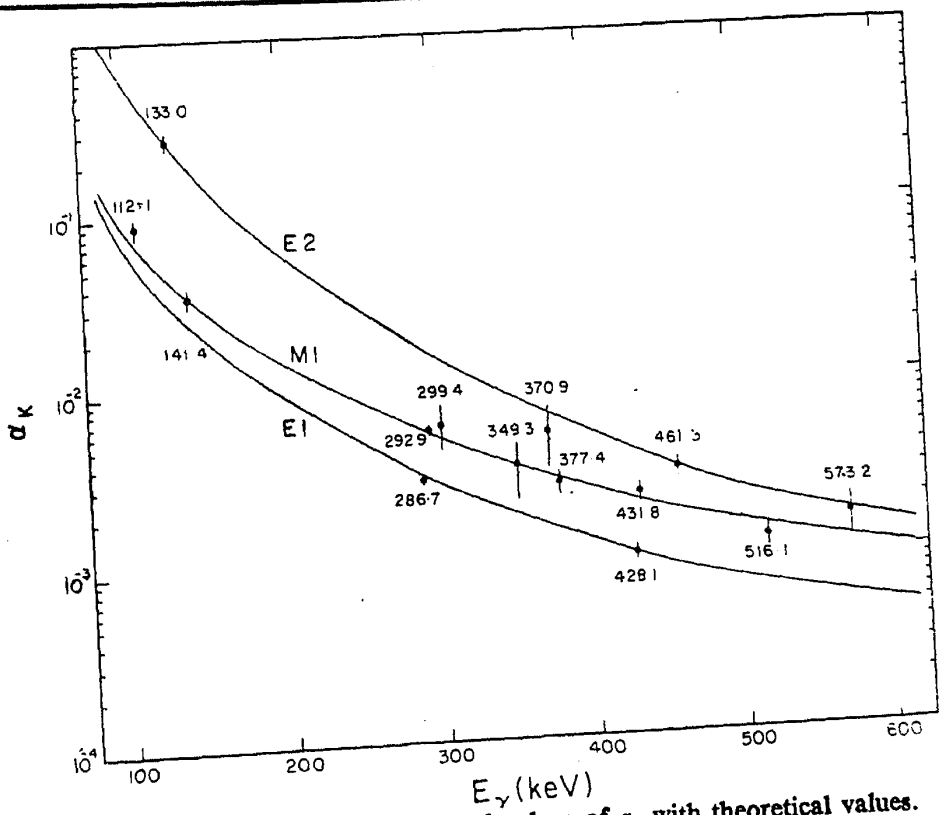


**Figure 2.** Comparison of the measured values of $\alpha_K$ with theoretical values. The continuous lines are the values of $\alpha_K$ taken from Hager and Seltzer (1968) for various multipolarities.

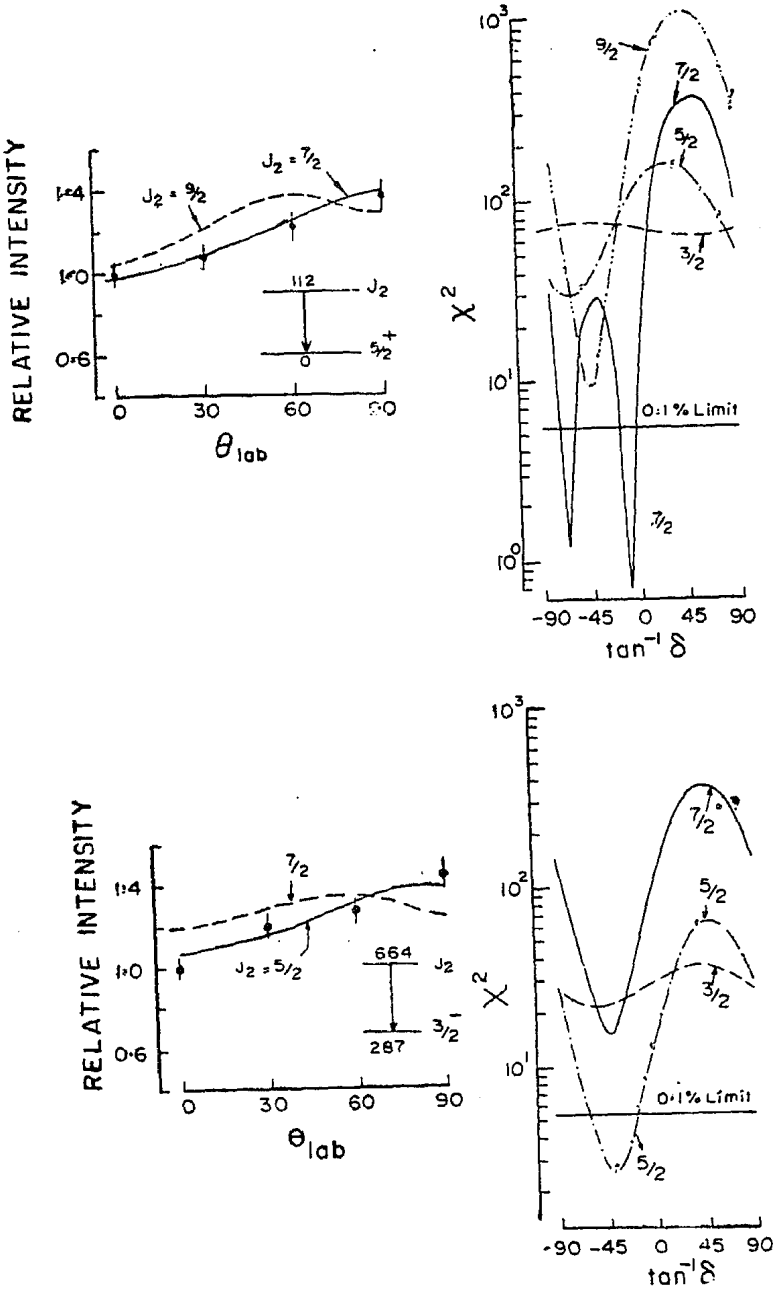


**Figure 3.** Angular distribution and $\chi^2$ plots for the 112·1 and 377·4 keV $\gamma$-rays. The lines through the angular distribution plots are the theoretical curves obtained by minimizing $\chi^2$ with respect to the mixing ratio $\delta$, for the indicated values of spin of the level.

and $\gamma$–$\gamma$ coincidence measurements, a level scheme of $^{75}$Se shown in figure 4 is proposed. The results of earlier measurements have also been used in assigning the spins and parities of the levels. In the present work, unambiguous assignments of spins and parities to most of the levels below 750 keV have been made. Further, the multipolarities of many of the transitions among these levels have also been determined and are shown in figure 4. The individual levels are discussed in detail in the following sections.

### 3.1. *Ground state*

This state is known to have a spin $5/2^+$ and a large quadrupole moment $Q = 1{\cdot}1$ barn (Aamadt and Fletcher 1955).

**Table 2.** Summary of coincidence measurements

| Window width (keV) | $E_\gamma$ in gate (keV) | $E_\gamma$ in coincidence (keV) |
|---|---|---|
| 88–124 | 112·1 | 20·9[a], 211·7, 236·0, 285·0, 316·0, 319·7, 349·4, 431·8, 495·4, 516·1, 534·6, 552·2, 630·2, 657·2, 678·0, 761·2, 770·4, 873·4, 891·6, 962·4, 978·5, 1048·7, 1076·9, 1188·9. |
| 118–162[b] | 133·0, 141·4 | 236·0, 286·7, 319·7, 349·4, 431·8, 495·4, 534·6, 657·2, 761·2, 770·4. |
| 256–326 | 285·0, 286·7, 292·9, 299·4, 316·0, 319·7 | 6·5[c], 112·1, 141·4, 191·1, 236·0, 292·9, 299·4, 316·0, 319·7, 349·4, 377·4, 428·1, 431·8, 461·3, 490·6, 534·6, 566·2, 573·2, 598·4, 609·1, 657·2, 676·1, 678·0, 734·1, 761·2, 770·4, 873·4, 897·4, 912·0, 951·8, 978·5. |
| 495–530 | 490·6, 495·4, 516·1 | 112·1, 133·0, 211·7, 286·7, 630·2 |

(*a*) Obtained from data in figure 6.
(*b*) With this gate, the coincidence spectrum measured extends up to 800 keV only.
(*c*) Obtained from data in figure 7.

### 3.2. *The* 112·1 *keV state*

The angular distribution of the 112·1 keV $\gamma$-ray and the value of its $\alpha_k$ establish the spin of the 112·1 keV state as $7/2^+$. The E2/M1 mixing ratio of the 112·1 keV $\gamma$-ray was determined from its $\alpha_k$ value, K/L ratio and angular distribution data to be $4 \pm 2\%$. The half-life was determined to be $0{\cdot}69 \pm 0{\cdot}12$ nsec; in this measurement the K-conversion line of the 112·1 keV-transition was used as "start" for the TAC and the 516·1 keV transition was used as 'stop'. The resulting time spectrum is shown in figure 5.

### 3.3. *The* 133·0 *keV state*

The internal conversion electron spectrum (figure 1) shows a strong conversion line of energy 120 keV. The line was established to be the K-conversion line of a weak 133·0 keV $\gamma$-ray in $^{75}$Se on the basis of the energies of the $\gamma$-ray and the internal conversion electron line. While the excitation function of the K 133·0 keV conversion line shows that this transition originates from a level of energy less than 500 keV, it was established to be a transition from a level at 133·0 keV from the $e_k - \gamma$ and $\gamma$–$\gamma$ coincidence experiments and the threshold energies of the coincident $\gamma$-rays. The $\alpha_k$ for this transition requires it to be E2 in nature and thus the spin of the 133·0 keV level is probably $1/2^+$ or $9/2^+$. The former value can be ruled out from the absence of a transition from the 286·7 keV $(3/2^-)$ state to this state and the absence of electron capture decay to this state from the ground state of $^{75}$Br (Coban *et al* 1972). The relatively high proton energy at which the 133·0 keV transition was first observed also supports the $9/2^+$ assignment. This state is expected to decay to the 112·1 keV state through a 20·9 keV transition which should have a multipolarity M1 + (E2). To confirm this, a $\gamma$-ray spectrum

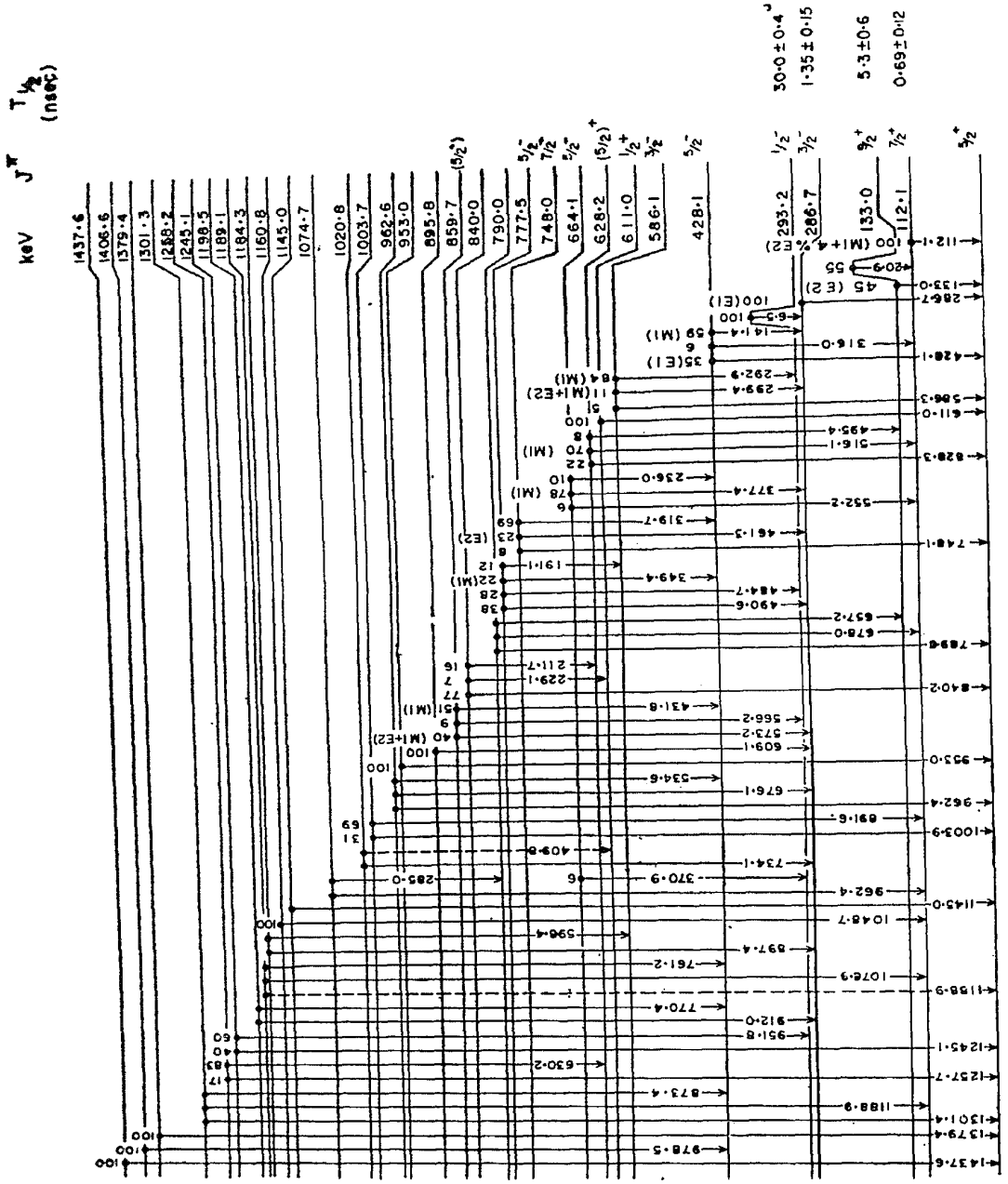


**Figure 4.** Proposed level scheme of $^{75}$Se. The branching ratios and the multipolarities wherever determined are indicated on the top of the corresponding transitions. The half-life for the 293·2 keV state is taken from Richter *et al* (1968).

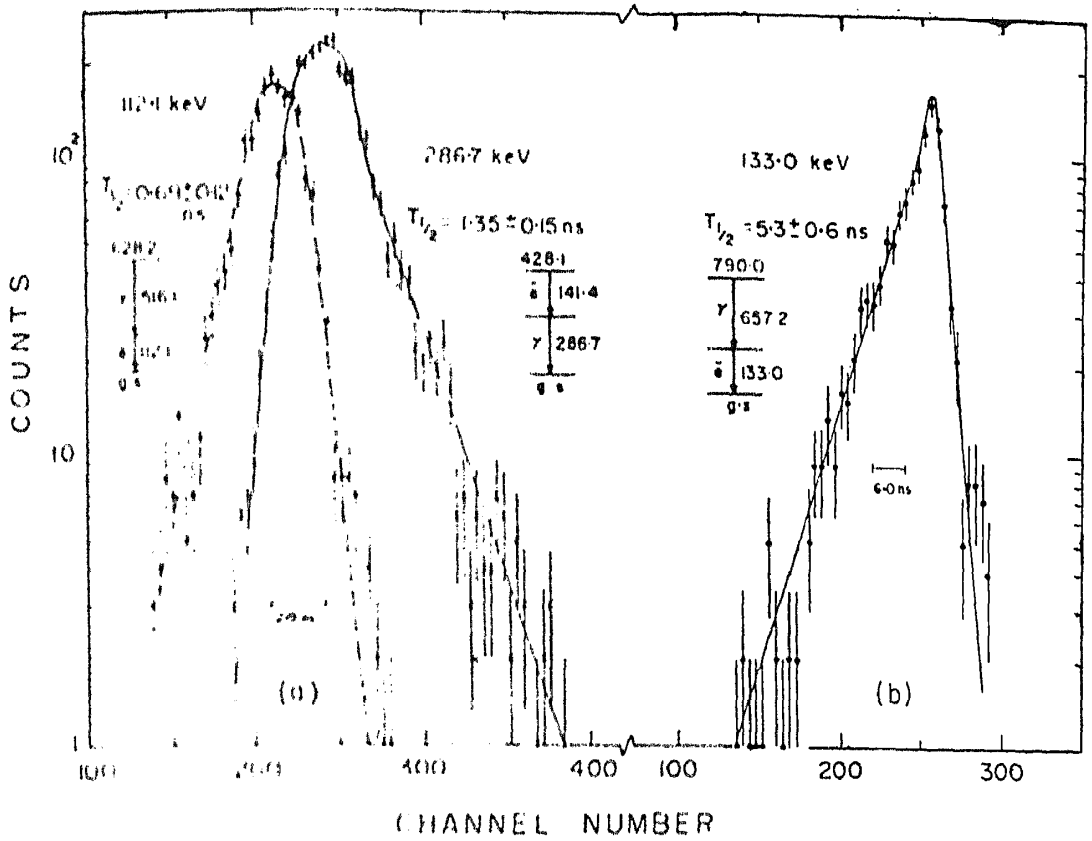


Figure 5. The decay curves for (*a*) 112·1 and 286·7 keV levels, (*b*) 133·0 keV level. The radiations used for the measurements are also shown in the figures. For the 112·1 keV time spectrum, the left side of the 286·7 keV time spectrum gives the prompt slope while for the 286·7 keV time spectrum the right side of the 112·1 keV time spectrum gives the prompt slope.

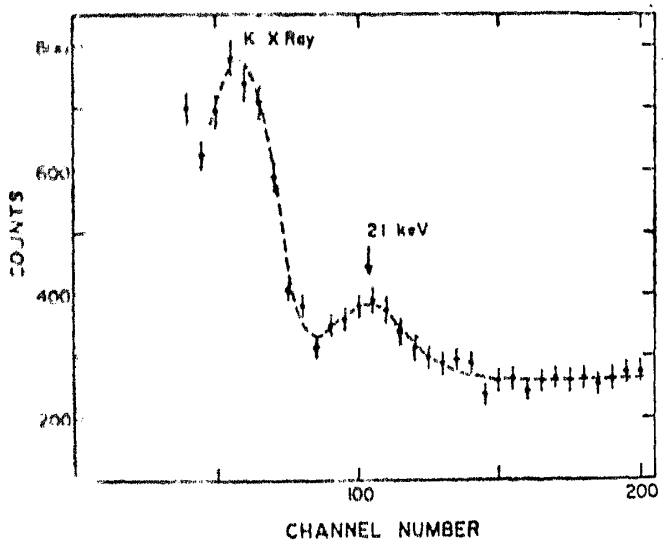


Figure 6. The $\gamma$-$\gamma$ coincidence spectrum at $E_p = 4{\cdot}0$ MeV in the range 10–30 keV taken with a thin window NaI (Tl) detector gated by a $110 \pm 20$ keV $\gamma$-ray window chosen in another NaI (Tl) detector.

was taken at $E_p$ 4·0 MeV, with a thin window Ge (Li) detector made in our laboratory and this showed a $\gamma$-line at $21{\cdot}0 \pm 0{\cdot}5$ keV. Further, a coincidence spectrum with a thin window NaI (Tl) detector, gated by the 112·1 keV $\gamma$-ray was also recorded in order to confirm this transition. The coincidence spectrum is shown in figure 6 and it unambiguously shows that the 133·0 and 20·9 keV

transitions originate from a level at 133·0 keV. From the known relative efficiency of the Ge (Li) detector, the ratio of the intensities of the 20·9 and 133·0 keV $\gamma$-rays was found to be $0{\cdot}14 \pm 0{\cdot}05$. In order to obtain information about $\gamma$-transitions feeding the 133·0 keV level, a $\gamma$-ray spectrum in a NaI (Tl) detector was recorded in coincidence with the K-conversion line of the 133·0 keV transition. The resulting spectrum showed that the 495·4 and 657·2 keV $\gamma$-rays are in coincidence with the 133·0 keV transition. The half-life of this state was measured using the 657·2 keV ($\gamma$)—133·0 keV ($e_K$) cascade. The time spectrum is shown in figure 5 and the half-life was found to be $5{\cdot}3 \pm 0{\cdot}6$ nsec. This value was confirmed by a measurement of the time spectrum between neutrons (detected in a 5 cm × 5 cm plastic detector with a 3 cm thick lead absorber in front) and the K-133·0 keV conversion line. After this work had been completed, Sanderson (1973) reported a study of the reaction $^{76}$Se(d, t)$^{75}$Se in which a level at 133 keV with a transferred $l = 4$ was seen. This is in agreement with the present spin assignment.

### 3.4. *The* 286·7 *and* 293·2 *keV levels*

The E1 nature of the 286·7 keV $\gamma$-ray (figure 4) and the absence of a transition from the 286·7 keV level to the 112·1 keV ($7/2^+$) level indicate that the spin of this level is $3/2^-$. Several measurements of the half-life of this level have been reported. While Tubbs (1966) reported a value $T_{1/2} \simeq 1{\cdot}0$ nsec and Ray *et al* (1969) on the basis of the $e^+ - \gamma$ delayed coincidence measurements gave a value $T_{1/2} = 1{\cdot}23 \pm 0{\cdot}15$ nsec, Richter *et al* (1968) reported a value $T_{1/2} = 30{\cdot}0 \pm 0{\cdot}4$ nsec. This disagreement was clarified by the work of Coban *et al* (1972) who showed that the 286·7 keV transition displays both the half-lives. They observed that if the level was populated by the 141·4, 377·4, 573·2, 609·1, 734·1 and 912·1 keV $\gamma$-rays, a short half-life resulted, but a much longer half-life ($T_{1/2} = 29{\cdot}6 \pm 3{\cdot}2$ nsec) was measured when the level was populated by the 292·9 and 952·1 keV transitions. On the basis of these results, they concluded that two close lying levels separated by less than 1 keV are located at 286·7 keV and that they both decay to the ground state with $\gamma$-rays of energies too close to be resolved by their detectors. A spin ($3/2^-$, $5/2^-$) was assigned by Coban *et al* (1972) to both these levels as the 286·7 keV $\gamma$-ray was found to have a multipolarity E1. It is tempting to place a level at 292·9 keV on the basis of observation of a $\gamma$-ray of this energy. However this possibility is ruled out on the basis of the observation by Coban *et al* (1972) and in the present work that the 286·7 keV and the 292·9 keV transitions are in coincidence with each other. Richter *et al* (1968), using a pulsed beam showed that the 292·9 keV transition does not follow a long ($\simeq$ 30 nsec) half-life. The observed threshold values, 2·1 and 2·3 MeV respectively for the 286·7 keV and 292·9 keV $\gamma$-rays also rule out this possibility.

A more plausible explanation of the above mentioned observations would be to postulate a state with spin $1/2^-$ and with the longer half-life at an energy slightly higher than the 286·7 keV ($3/2^-$) state which has the shorter half-life, the $1/2^-$ state decaying only to the 286·7 keV ($3/2^-$) state by an M1 transition. This would explain the absence of any $\gamma$-ray other than the 286·7 keV transition following the 30 nsec half-life. Further support for this explanation is provided by the fact that in the level scheme proposed by Coban *et al* (1972), there are no fewer than six $\gamma$-ray doublets, all separated by $6{\cdot}2 \pm 0{\cdot}5$ keV and in coincidence with the 286·7

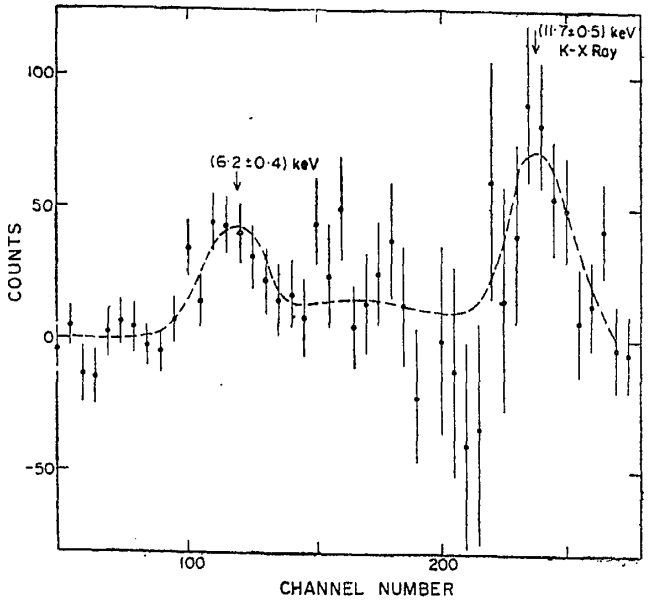


**Figure 7.** The spectrum taken with a Kr-filled proportional counter gated by $290 \pm 20$ keV $\gamma$-ray window selected in a NaI (Tl) detector with resolving time $\simeq 2\mu$ sec.

keV $\gamma$-ray. If the proposed level is $6{\cdot}2 \pm 0{\cdot}5$ keV higher than the 286·7 keV level, the six doublets of levels proposed by Coban *et al* (1972) are reduced to six levels and the six doublets of transitions would then be transitions from these six levels to the 286·7 keV and the $286{\cdot}7 + (6{\cdot}2 \pm 0{\cdot}5)$ keV levels.

In order to verify this explanation, a measurement was made of the $\gamma$-rays in the energy range 3–20 keV in coincidence with 286·7 keV $\gamma$-ray. The low energy $\gamma$-rays were detected in a krypton filled proportional counter and the 286·7 keV $\gamma$-ray was detected in a NaI (Tl) detector. Due to the very intense As X-rays produced by the incident protons knocking off the K-electrons from As atoms and the large resolving time ($2\tau = 2\mu$s) that resulted from the use of the proportional counter, a proton beam of a few nA had to be used for this measurement. The resulting coincidence spectrum, corrected for chances, is shown in figure 7. In addition to K x-rays from Se, a $\gamma$-ray of energy $6{\cdot}2 \pm 0{\cdot}4$ keV is clearly seen in this spectrum. This experiment thus clearly shows that there exist two levels one at 286·7 keV ($3/2^-$) and the other at 293·2 keV ($1/2^-$). The arguments for the spin assignments were given earlier. The half-lives of both the states were also measured. For the 286·7 keV state, the cascade used was 141·4 keV ($e_K$)–286·7 keV ($\gamma$) and the result is shown in figure 5. The half-life was found to be $T_{1/2} = 1{\cdot}35 \pm 0{\cdot}15$ nsec in agreement with the value reported by Ray *et al* (1969). The half-life of the 293·2 keV state was measured by using two NaI (Tl) detectors and selecting broad windows around 280 keV in both. A value in good agreement with the value given by Richter *et al* (1968) was obtained.

### 3.5. *The* 428·1 *keV state*

The 428·1 keV state was established on the basis of coincidence between the 141·4 and 286·7 keV $\gamma$-rays, the 428·1 keV cross-over $\gamma$-transition and threshold measurements. The 141·4 and 428·1 keV transitions from this level are found to

be M1 and E1 respectively and therefore this state can have a spin $3/2^-$ or $5/2^-$. The angular distribution of the 141·4 keV $\gamma$-ray (*see* section 2.4) rules out a $3/2^-$ assignment leaving $5/2^-$ as the only possible spin. The value $3/2^-$ is also ruled out on the basis of the observation of a 316·0 keV transition from the 428·1 keV state to the 112·1 keV ($7/2^+$) state.

### 3.6. *The* 586·1 *keV state*

Three transitions from this state to the ground state, the 286·7 and 293·2 keV states have been observed along with the expected coincidence relationships. The 292·9 keV $\gamma$-ray has a sharp threshold at $E_p = 2{\cdot}3$ MeV. The 292·9 and 299·4 keV transitions were found to be M1 and M1 + E2 respectively. The presence of the ground state transition rules out a $1/2^-$ assignment for this level. These observations suggest a spin $3/2^-$ for the 586·1 keV state. This assignment is supported by the fact that this level is populated in the electron capture decay of $^{75}$Br (Coban *et al* 1972) and by the absence of a transition to the 112·1 keV ($7/2^+$) state.

### 3.7. *The* 611·0 *keV state*

This level has been established on the basis of the threshold of the 611·0 keV $\gamma$-ray. Our angular distribution results for this $\gamma$-ray were not conclusive. However Sanderson (1973) has assigned a spin $1/2^+$ to this state on the basis of the angular distribution of tritons in the reaction $^{76}$Se(d, t)$^{75}$Se. This spin assignment is supported by the absence of transitions from this state to the $7/2^+$ and $9/2^+$ levels at 112·1 and 133·0 keV respectively.

### 3.8. *The* 628·2 *keV state*

The angular distribution of the 628·2 keV $\gamma$-ray suggests a range of spins 3/2 to 9/2. The M1 character of the 516·1 keV transition to the 112·1 keV ($7/2^+$) state indicates a positive parity for this state. On the basis of the existence of transitions from this state to the 112·1 keV ($7/2^+$), 133·0 keV ($9/2^+$) and the ground ($5/2^+$) states and also the small branching to the 133·0 keV state, the assignment $5/2^+$ is favoured.

### 3.9. *The* 664·1 *keV state*

Four transitions from this state to the 112·1, 286·7, 293·3 and 423·1 keV states have been established on the basis of the threshold and $\gamma$–$\gamma$ coincidence measurements. The angular distribution results and the M1 nature of the 377·4 keV transition from this state to the 286·7 keV ($3/2^-$) state require a spin value $5/2^-$ for this state.

### 3.10. *The* 748·0 *keV state*

Three transitions from this state to the 286·7 keV, 428·1 keV and the ground states have been observed. The multipolarity of the 461·3 keV transition to the 286·7 keV ($3/2^-$) level is found to be E2 and thus the spin of this level is $7/2^-$.

### 3.11. *The higher states*

Most of the higher levels shown in figure 4 have been reported earlier; however the states at 953·0 and 1258·2 keV are proposed here on the basis of the $\gamma$–$\gamma$ coincidence and $\gamma$-ray excitation function data. The branching ratios for these and

the other high-lying levels have been obtained and are shown in figure 4. The errors in the branching ratios are 10–20%.

### 3.12. *Reduced transition probabilities*

From the measured values of half-lives and the known multipolarities of the different transitions as determined here, the reduced transition probabilities for some of the low-lying transitions were determined. In these calculations the 6·5 and the 20·9 keV transitions were assumed to be pure M1 and the total conversion coefficient values were taken from Hager and Seltzer (1968). The calculated values are given in table 3 along with Weisskopf estimates (Bohr and Mottelson 1969) and the results of the recent theoretical calculations by Ikegami and Sano (1973). From the table, it can be seen that the $7/2^+ \rightarrow 5/2^+$ and $9/2^+ \rightarrow 7/2^+$ M1 transitions are retarded while the $9/2^+ \rightarrow 5/2^+$ and $9/2^+ \rightarrow 7/2^+$ E2 transitions are enhanced.

## 4. Discussion

The spins and parities of the levels up to 748 keV excitation energy have been unambiguously determined as outlined above. In the following the nature of the positive and negative parity levels will be discussed separately.

Positive parity levels. According to the single particle shell model, the valence neutrons have only the $g_{9/2}$ orbital available in this region to give rise to positive parity states. The nearest positive parity states are the $d_{5/2}$ and $g_{7/2}$ and these are much higher in energy, above the neutron shell closure at $N = 50$. Thus one expects that all the low-lying positive parity levels originate from the coupling of the $g_{9/2}$ neutron to various core configurations. The $9/2^+$ level at 133·0 keV has been identified here and by Sanderson (1973). In addition, low-lying $5/2^+$ and $7/2^+$ states are seen and these are even lower than the $9/2^+$ level. The simplest way to obtain the $5/2^+$ and $7/2^+$ states would be by coupling the $g_{9/2}$ to the $2^+$ states of the even-even core, *viz.*, $(g_{9/2} \times 2^+)_{5/2^+,\ 7/2^+}$. In this description however it is difficult to understand the lowering of the energy of the $7/2^+$ and $5/2^+$ states. Similar $7/2^+$ states, quite low in energy, have been observed in neighbouring odd N nuclei.

**Table 3.** Reduced transition probabilities of low-lying transitions in $^{75}$Se

| Transition (keV) | Multi-polarity | Reduced transition probabilities | | |
|---|---|---|---|---|
| | | Observed[a] | Calculated[a] Ikegami and Sano | Observed (Weisskopf units) |
| 112·1 | M1 | (3·6±0·7) × (−2) | 3·6 × (−1) | (2·0±0·4) × (−2) |
| | E2 | (1·7±0·9) × (+3) | 3·8 × (+2) | 90±40 |
| 133·0 | E2 | (7·9±2·0) × (+2) | 6·3 × (+2) | 42±11 |
| 20·9 | M1 | (4·6±0·7) × (−2) | 1·98 | (2·6±0·4) × (−2) |
| 286·7 | E1 | (1·3±0·2) × (−5) | .. | (1·1±0·2) × (−5) |
| 6·5 | M1 | 0·11 | .. | 0·063 |

(*a*) B (E2), B (M1) and B (E1) are expressed in units of $e^2fm^4$, $(n.m)^2$ and $e^2fm^2$ respectively.

Sherwood and Goswami (1966) and Goswami and Nalcioglu (1967) extended the quasi-particle phonon coupling model of Kisslinger and Sorensen (1963) in order to explain the occurrence of the low-lying $5/2^+$ level in $^{75}$Se in their so-called EQPC model, where they consider also the coupling to the backward going amplitudes. This has the effect of pushing the $9/2^+$ quasi-particle level to the vicinity of the phonon level. Further, the $5/2^+$ phonon level comes down relative to the other phonon levels especially at the beginning of the $g_{9/2}$ shell, due to the de-Shalit self-energy term for a large negative quadrupole moment of the phonon state. Even though Goswami and Nalcioglu (1967) explained the lowering of the $5/2^+$ level, they did not calculate the reduced transition probabilities between the low lying positive parity states.

Ikegami and Sano (1966, 1973) have improved upon the QPC (Kisslinger and Sorensen 1963) picture by including large number of shells and more phonon states and introducing a spin-quadrupole interaction. In table 3, the reduced transition probabilities calculated by them are compared with the experimental values. The agreement with the experiment in the case of $B$ (E2) values is reasonably good, but for $B$ (M1) values there is a gross disagreement.

An alternative way of explaining the results, in particular the large $B$ (E2) values and the large ground state quadrupole moment, may be in terms of deformation. It should, however, be noted that while there are well developed negative parity rotational bands (*see* below), the positive parity levels could not be fitted into simple rotational bands. Scholz and Malik (1968) have considered such deformed states with strong Coriolis interaction in their calculations of odd proton nuclei in this region. Sanderson (1973) has made similar Coriolis coupling model calculations for the positive parity levels in the odd neutron nucleus $^{75}$Se and finds that a reasonable agreement between the observed and calculated energy levels could be obtained for a deformation parameter $\beta_2 \simeq 0{\cdot}3$. There are several qualitative features apart from the large value of $B$ (E2) and the large ground state quadrupole moment that lend support to this picture. The 611·0 keV level has been assigned a spin value $1/2^+$. It is difficult to understand the occurrence of such a low-lying $1/2^+$ state on the basis of a simple core coupling model in which such a state can occur only by coupling the $g_{9/2}$ neutron to a two-phonon state. On the other hand, the $\Omega = 1/2^+$ band from the $d_{5/2}$ and $g_{7/2}$ states comes down in energy for prolate deformation. Further, Litvin *et al* (1968) found in their $^{76}$Se(d, p)$^{77}$Se work that there is a large $l = 2$ stripping strength to levels at quite low energy. This again implies a large admixture of the d-orbital which can come if the nucleus is prolately deformed. Recently Protop *et al* (1973) have excited high spin states in $^{75}$Se through ($\alpha$, xn) reactions on Ge isotopes. They find a $K = 3/2^-$ rotational band built on the 287 keV level and also a number of high spin positive parity states. Though the spin assignments are not unique, they suggest that the high spin positive parity levels form a ' decoupled band ' built on the $9/2^+$ state. Such bands are seen in other nuclei also and are expected when there is a high $j$ state near the Fermi level in a deformed nucleus and large Coriolis coupling is favourable (Stephens *et al* 1972). These evidences thus show that a qualitative understanding of the positive parity levels is achieved on the basis of a deformation for $^{75}$Se.

Negative parity states. The negative parity states in $^{75}$Se and the neighbouring odd-neutron nuclei have been discussed by Baba *et al* (1974) with the suggestion that these can be understood again on the basis of a deformation with $\beta_2 = 0{\cdot}35$.

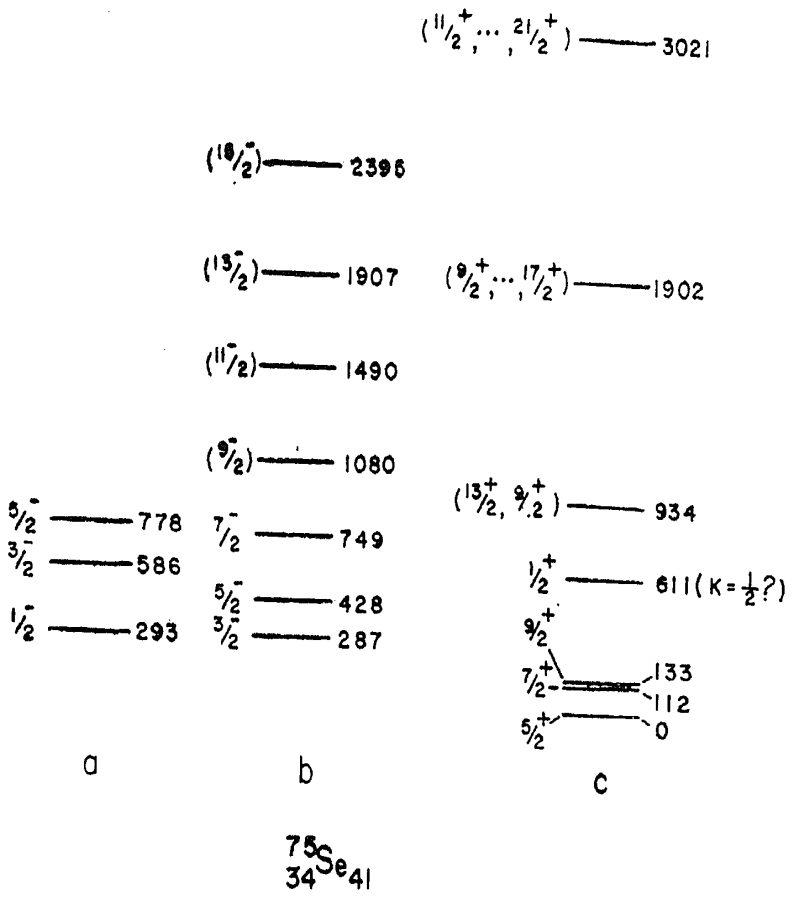


**Figure 8.** Summary of the energy levels of $^{75}$Se. Levels 'a' form the $K = 1/2^-$ rotational band and levels 'b' constitute the $K = 3/2^-$ band. Among the positive parity levels 'c', the 133, 934, 1912 and 3021 keV levels might form a decoupled band based on the $9/2^+$ state.

The main reasons for this conclusion are (i) the 293·2 keV ($1/2^-$), 586·1 keV ($3/2^-$) and 748·0 keV ($5/2^-$) levels in $^{75}$Se and similar levels in $^{77}$Se and $^{79}$Kr can be fitted in a rotational band, (ii) the observation of a $K = 3/2^-$ band with the 287·6 keV ($3/2^-$) state as the band head (Protop *et al* 1973), (iii) the large $B$(E2) values of the $2^+ \rightarrow 0^+$ transitions in the neighbouring even-even Se and Kr isotopes and the large ground state quadrupole moments for $^{75, 79}$Se, (iv) the observation of rotational-like spectrum in the neighbouring even-even Kr and Se isotopes for states having spins more than $6^+$, (v) the calculations of Tanaka and Tomoda (1973) where a minimum for the potential energy is obtained for $\beta_2 = 0{\cdot}35$.

In figure 8 some of the levels of $^{75}$Se observed in the present work and by Protop *et al* (1973) are summarized. The levels are separated into different bands: the $K = 1/2^-$, $K = 3/2^-$ negative parity rotational bands and the possible positive parity decoupled band.

In conclusion, the negative parity levels in $^{75}$Se can be understood rather well if the nucleus is deformed with a deformation parameter $\beta_2 \simeq 0{\cdot}35$. The positive parity levels can also be understood on the basis of deformation, albeit qualitatively.

## Acknowledgements

The authors wish to thank Professor K M Bisgaard of the Physics Laboratory, Royal Veterinary and Agricultural University, Copenhagen, for advice in building

the six-gap spectrometer and supplying the parts. Thanks are due to Dr. K V K Iyengar, S K Amberdekar, P J Bhalerao, M D Deshpande, M G Patwardhan, S C Vaidya, M Y Vaze and Kum. K H Umadiker for help in various phases of the work. The authors would also like to thank the Van de Graaff operation staff for running the machine efficiently.

## References

Aamadt L C and Fletcher P C 1955 *Phys. Rev.* **98** 1224
Agarwal Y K, Bharathi S M, Bhattacherjee S K, Lal B, Sahai B and Baba C V K 1973 *Proc. Int. Conf. Nucl. Phys.* eds J de Boer and H J Mang (North-Holland, Amsterdam) **1** 288
Amberdekar S K, Bharathi S M and Baba C V K 1969 *Proc. Nucl. Phys. Solid State Phys. Symp. Roorkee* Vol. II, 266
Auerbach E H 1964 ABACUS-2 Program operation and input description, Brookhaven National Laboratory Report No. BNL 6562
Baba C V K, Bharathi S M and Lal B 1974 *Pramāṇa* **2** 239
Bisgaard K M 1963 *Nucl. Instrum. Methods* **22** 221
Bohr A and Mottelson B R 1969 *Nuclear structure* (W A Benjamin Inc., New York) 389
Coban A, Willmott J C, Lisle J C and Murray G 1972 *Nucl. Phys.* A **182** 385
Deshpande M D 1971 M.Sc. Thesis, Bombay University
Dzhelepov B C, Dmitriev A G, Zhukovskii N N, Moskvin L N and Penionzhkevich Yu E 1969 *Bull. Acad. Sci. USSR Phys. Ser.* **33** 1513
Dzhelepov B C, Dmitriev A G, Zhukovskii N N, Mozzhukhin A V and Fominykh V I 1970 *Bull. Acad. Sci. USSR Phys. Ser.* **34** 1845
Finckh E, Jahnke U, Schreiber B and Weidinger A 1970 *Nucl. Phys.* A **144** 37
Goswami A and Nalcioglu O 1968 *Phys. Lett.* **26B** 353
Greenwood R C, Helmer R G and Gehrke R J 1970 *Nucl. Instrum. Methods* **77** 141
Hager R S and Seltzer E C 1968 *Nucl. Data* **A4** 1
Ikegami H and Sano M 1966 *Phys. Lett.* **21** 323
Ikegami H and Sano M 1973 *Proc. Int. Conf. Nucl. Moments Nucl. Structure* eds H Horie and K Sugimoto (Physical Society of Japan, Tokyo) 451
Kisslinger L S and Sorensen R A 1963 *Rev. Mod. Phys.* **35** 853
Ladenbauer-Bellis I M and Bakhru H 1969 *Phys. Rev.* **178** 2019
Lal B and Sahai B 1972 *Proc. Nucl. Phys. Solid State Phys. Symp. Bombay* **2** 27
Litvin V G, Nemilov Yu A, Zherebetsova K I *et al* 1968 *Bull. Acad. Sci. USSR Phys. Ser.* **32** 250
Protop C, Zell K-O, Friederichs H-G, Heits B and von Brentano P 1973 *Proc. Int. Conf. Nucl. Phys.* eds J de Boer and H J Mang (North-Holland, Amsterdam) **1** 216
Ray S, Mo T N, Muszynski S and Mark S K 1969 *Nucl. Phys.* A **138** 49
Richter P W, Schutt J and Wiegandt D 1968 *Z. Phys.* **217** 1
Rosen L, Beery J G and Goldhaber A S 1965 *Ann. Phys. (New York)* **34** 96
Routti J T and Prussin S G 1969 *Nucl. Instrum. Methods* **72** 125 and UCRL-19452 (unpublished)
Rudak E A, Firsov E I and Khil'Manovich D M 1970 *Sov. J. Nucl. Phys.* **11** 627
Sahai B and Lal B 1970 *Proc. Nucl. Phys. Solid State Phys. Symp. Madurai* **2** 1
Sanderson N E 1973 *Nucl. Phys.* A **216** 173
Sheldon E and Van Patter D M 1966 *Rev. Mod. Phys.* **38** 143
Scholz W and Malik F B 1968 *Phys. Rev.* **176** 1355
Sherwood A I and Goswami A 1966 *Nucl. Phys.* **89** 465
Stephens F S, Diamond R M, Leigh J R, Kammuri T and Nakai K 1972 *Phys. Rev. Lett.* **29** 438
Tanaka Y and Tomoda T 1973 *Progr. Theor. Phys.* **50** 121
Tubbs N A 1966 Ph.D. Thesis, Oxford University (unpublished)
Wilmore D and Hodgson P E 1964 *Nucl. Phys.* **55** 673